Development/Plasticity/Repair

Temperature-Dependent Developmental Plasticity of *Drosophila* Neurons: Cell-Autonomous Roles of Membrane Excitability, Ca^{2+} Influx, and cAMP Signaling

I-Feng Peng,[1]* Brett A. Berke,[2]* Yue Zhu,[1] Wei-Hua Lee,[1] Wenjia Chen,[1] and Chun-Fang Wu[1,2]

[1]Department of Biological Sciences and [2]Interdisciplinary Program in Neuroscience, University of Iowa, Iowa City, Iowa 52242

Environmental temperature is an important factor exerting pervasive influence on neuronal morphology and synaptic physiology. In the *Drosophila* brain, axonal arborization of mushroom body Kenyon cells was enhanced when flies were raised at high temperature (30°C rather than 22°C) for several days. Isolated embryonic neurons in culture that lacked cell–cell contacts also displayed a robust temperature-induced neurite outgrowth. This cell-autonomous effect was reflected by significantly increased high-order branching and enlarged growth cones. The temperature-induced morphological alterations were blocked by the Na^+ channel blocker tetrodotoxin and a Ca^{2+} channel mutation but could be mimicked by raising cultures at room temperature with suppressed K^+ channel activity. Physiological analyses revealed increased inward Ca^{2+} currents and decreased outward K^+ currents, in conjunction with a distal shift in the site of action potential initiation and increased prevalence of TTX-sensitive spontaneous Ca^{2+} transients. Importantly, the overgrowth caused by both temperature and hyperexcitability K^+ channel mutations were sensitive to genetic perturbations of cAMP metabolism. Thus, temperature acts in a cell-autonomous manner to regulate neuronal excitability and spontaneous activity. Presumably, activity-dependent Ca^{2+} accumulation triggers the cAMP cascade to confer the activity-dependent plasticity of neuronal excitability and growth.

Key words: **mushroom body; Kenyon cells; growth cones; nerve terminal arborization; K^+ channels; Ca^{2+} channels; action potential; Ca^{2+} transients/dynamics; spontaneous activity**

Introduction

Animals sense changes in environmental temperature using specific sensory transduction and neural pathways and respond with a variety of behaviors. The molecular and cellular mechanisms required for sensing and responding to cold and heat have been studied extensively in genetic model systems such as *Caenorhabditis elegans* (Samuel et al., 2003; Kimura et al., 2004) and *Drosophila* (Tracey et al., 2003; Lee et al., 2005; Rosenzweig et al., 2005; Hong et al., 2006). However, temperature also has pervasive, nonspecific effects on gene expression, enzyme activity, and ion channel kinetics in individual neurons, resulting in physiological and developmental alterations that may be important to animal adaptation and survival.

It is known that acute temperature shifts modulate short-term synaptic plasticity in the hippocampus, the spinal cord, and the calyx of Held (Klyachko and Stevens, 2006; Kushmerick et al., 2006; Wan et al., 2006). In contrast, chronic temperature changes affect neuronal development, leading to morphological alterations. For example, dendritic spines are retracted in the hippocampus of the ground squirrel during cold temperature-induced hibernation (Popov and Bocharova, 1992; Popov et al., 1992) and in mouse brain slices when exposed to a prolonged temperature decrease (Kirov et al., 2004). In honey bees, slight deviations in brood temperature during pupation strongly influence the architecture of olfactory circuits (Groh et al., 2004) and perturb memory acquisition and retention (Tautz et al., 2003; Jones et al., 2005). At the well characterized *Drosophila* larval neuromuscular junction, axon terminal arborization and neurotransmission are both enhanced when animals develop at an increased temperature (Sigrist et al., 2003; Zhong and Wu, 2004). These temperature effects seem to be mediated by an increase in presynaptic excitability (Zhong and Wu, 2004), reminiscent of the enhanced motor axon ramification in hyperexcitable K^+ channel mutants (Budnik et al., 1990; Zhong et al., 1992). However, at elevated temperatures, enhanced neuronal growth may result from trophic interaction involving both central pattern generator activity and muscle contraction (Sigrist et al., 2003; Steinert et al., 2006). Hence, it is important to delineate cell-autonomous components from those requiring cell–cell interactions in temperature-dependent neuronal plasticity.

Cell-autonomous effects of environmental temperature on neuronal development can be readily addressed through a com-

Received May 11, 2007; revised Sept. 6, 2007; accepted Sept. 27, 2007.

This work was supported by National Institutes of Health Grants HD18577 and NS26528. We thank Jihye Lee for advice on confocal microscopy. We also thank Haig Keshishian and Yale University for the use of their confocal microscopy facilities.

*I-F.P. and B.A.B. contributed equally to this work.

Correspondence should be addressed to Dr. Chun-Fang Wu, Professor, Department of Biological Sciences, University of Iowa, Iowa City, IA 52242. E-mail: chun-fang-wu@uiowa.edu.

I-F. Peng's present address: Department of Ophthalmology, University of California at San Francisco, San Francisco, CA 94143.

B. A. Berke's present address: Department of Molecular, Cellular, and Developmental Biology, Yale University, New Haven, CT 06520.

DOI:10.1523/JNEUROSCI.2179-07.2007

 0270-6474/07/2712611-12$15.00/0

bination of cell culture and *in vivo* analyses. By using the GAL4-UAS system (Brand and Perrimon, 1993), we demonstrate that high temperature induces overgrowth of mushroom body (MB) nerve terminals in the CNS, similar to the response seen at the peripheral neuromuscular junction (Zhong and Wu, 2004). A robust overgrowth was also observed in isolated neurons in embryonic cultures, including those from the MB lineage. In this study, we investigated the roles of ion channels, neuronal excitability, Ca^{2+} regulation, and signal transduction pathways in temperature-dependent plasticity of neuronal growth.

Materials and Methods

Fly strains. The Canton S strain was used as the wild-type (WT) control. Mutations affecting K^+ channel α subunits included several *ether a go-go* alleles (eag^1 and eag^{4PM}) and *Shaker* alleles (Sh^5, Sh^{133}, and Sh^M), as well as two *eag Sh* double mutants (eag^1Sh^{133} and $eag^{4PM}Sh^{120}$) (Ganetzky and Wu, 1983; Wu et al., 1983; Wu and Haugland, 1985; Haugland and Wu, 1990; Zhong and Wu, 1993; Peng and Wu, 2007a). A Ca^{2+} channel mutant, *cacophony* (cac^s), was examined (Peng and Wu, 2007b). Mutations affecting cAMP metabolism included *dunce* (dnc^1), which is defective in a cAMP-dependent phosphodiesterase (PDE), and *rutabaga* (rut^1 and rut^2), which is defective in an adenylate cyclase (AC) (Dudai et al., 1976; Byers et al., 1981; Livingstone et al., 1984; Tully and Quinn, 1985).

To visualize MB terminals, a chromosome carrying both the 201Y-Gal4 driver (O'Dell et al., 1995; Yang et al., 1995; Ito et al., 1997) and the UAS responder construct containing a membrane-bound CD8 fragment tagged with green fluorescent protein (UAS-mCD8-GFP) was obtained by recombination. This enables visualization of GFP-labeled MB Kenyon cells against different genetic backgrounds (WT, *eag*, or *rut*) after crosses with appropriate stocks. For the rescue experiment shown in Figure 10, targeted expression of UAS-Rut+ (Liu et al., 2006) was driven by 201Y-Gal4 in the rut^1 mutant background. Two additional UAS lines, expressing a GFP-tagged α tubulin (UAS-GFP-α-tub; stock number 7373; Bloomington Stock Center, Bloomington, IN) and a GFP-tagged non-muscle moesin actin-binding domain (UAS-GMA) (Bloor and Kiehart, 2001), were used to illustrate microtubule and actin filament structures after expressing them with the pan-neuronal $elav^{C155}$-Gal4 driver.

Confocal microscopy and analysis of terminal arborization of adult MBs. For testing the effects of high temperature, flies were raised at 30°C 1 d after eclosion, and control flies were raised at room temperature (RT; 22–23°C) throughout development. The fly brains of identified ages were removed in PBS, fixed in PBS containing 3.7% formaldehyde for 20 min, and subsequently rinsed with PBST (0.1% Triton X-100 in PBS) three times. The samples were further cleaned with the Focus Clear agent for 5 min and mounted with Mount Clear agent (both from Cedarlane Laboratories, Burlington, Ontario, Canada). A stack of MB images in 2 μm sections were taken with a 63× objective lens [numerical aperture (N.A.) 1.3] and a confocal microscope (model 1024; Bio-Rad, Hercules, CA). Three projections of Kenyon cells give rise to five axon lobes of the MB (α, α', β, β', and γ), and only subsets of neurons in α, β, and γ lobes are labeled with the 201Y-Gal4 driver (O'Dell et al., 1995; Yang et al., 1995; Ito et al., 1997). To quantify the extent of the terminal arborization, we determined the ratio of the axonal terminal field diameter (TD) and the axonal bundle diameter (BD) for both α and β lobes. TDs were obtained from the average of the brightest and clearest three sections, usually occurring in the middle of the stack. BDs were taken from the average of three different positions along the bundle. All the measurements were done by using the LaserSharp software (Bio-Rad).

Single embryo "giant" neuron cultures. The giant neuron culture system has been described previously (Wu et al., 1990). Briefly, the interior of a gastrula was extracted with a glass micropipette and dispersed into a drop of culture medium on an uncoated coverslip. The culture medium contained 80% *Drosophila* Schneider medium and 20% fetal bovine serum (both from Invitrogen, Carlsbad, CA), with the addition of 200 ng/ml insulin, 50 μg/ml streptomycin, and 50 U/ml penicillin (all from Sigma, St. Louis, MO). To generate multinucleated giant neurons from neuroblasts, cytochalasin B (CCB; 2 μg/ml; Sigma) was added at the time of plating to arrest cytokinesis (Wu et al., 1990). CCB was subsequently removed by washing with CCB-free medium 1 d after plating. The disruptions of actin filaments were restored within 1 d after CCB washout, as indicated by regular phalloidin staining patterns in filopodia and lamellipodia (Berke et al., 2006). Giant neurons obtained by inhibiting neuroblast divisions display morphological and biochemical markers that would be expressed by their daughter cells because determination of such lineage-specific traits occurs before neuroblast divisions (Salvaterra et al., 1987; Wu et al., 1990; Saito and Wu, 1991; Berke and Wu, 2002). This is important because the *Drosophila* MB is derived from four embryonic neuroblasts that divide throughout the larval and pupal stages to produce the structure of the adult MB (Ito and Hotta, 1992; Lee et al., 1999). For testing the effects of high temperature, neurons were cultured at RT on the first day with CCB, and they either stayed at RT or were moved to a 30°C incubator after CCB washout. In drug pretreatment experiments, neurons were grown in CCB-containing medium for the first day and then in drug-containing but CCB-free medium from the second day onward [10 nM tetrodotoxin (TTX; Sankyo, Tokyo, Japan), 1 mM 4-aminopyridine (4-AP; Sigma), or 1 mM 8-Br-cAMPs (Calbiochem, La Jolla, CA)]. All cultures were grown in a humidified chamber.

Phase-contrast and fluorescent microscopy of cultured neurons. Cultured giant neurons were observed with a 100× objective lens (N.A. 1.3) on an inverted microscope (DM IRBE; Leica, Wetzlar, Germany). Phase and fluorescent images were captured by a high-sensitivity digital camera (C4742-95; Hamamatsu Photonics, Shizuoka Pref, Japan). In this study, the growth cone was defined as an enlarged terminal containing a lamellipodial structure. Growth cone area measurements include the relatively thick central domain but exclude the filopodia. Each growth cone was measured with NIH ImageJ software. The neurite terminals were classified into four types (T1–T4) based on their apparent complexity: T1 terminals are the simplest, without major branches and with only a few filopodia; T2 terminals have a single bifurcation; T3 terminals display either tertiary branching or multiple ($n \geq 2$) secondary branches; and T4 terminals, the most complex type, exhibit high-order branching usually decorated with a great number of filopodia. The arborization index used to quantify neurite terminal complexity for cultures of each genotype is defined as follows: [(number of T1 terminals × 1) + (number of T2 terminals × 2) + (number of T3 terminals × 3) + (number of T4 terminals × 4)]/total number of terminals. In sampling terminals, each monopolar and bipolar cell contributes to one and two counts, respectively. For multipolar cells, the three more complex branches were sampled.

Ca^{2+} imaging. The protocols for ratiometric imaging of intracellular Ca^{2+} with fura-2 have been described in detail previously (Berke and Wu, 2002; Berke et al., 2006). Briefly, cells were bathed in loading medium containing 4–6 μM fura-2-AM and 10–15 μl/ml pluronic acid in the dark at RT for 1.5–3 h. Bath saline contained (in mM) 128 NaCl, 2 KCl, 4 $MgCl_2$, 1.8 $CaCl_2$, and 35.5 sucrose and was buffered at pH 7.1–7.2 with 5 HEPES (adjusted with NaOH). The 4 mM K^+ saline was identical but contained 4 mM KCl and 126 mM NaCl. Imaging was performed with an intensified CCD camera and a shutter/filter wheel controlled by the Ion Wizard software (Ion Optix, Milton, MA). The estimated K_D was 147 nM, obtained with a 100× objective, using a cell-free calibration (Williams et al., 1985; Berke et al., 2006). The Ca^{2+} level was quantified by applying the Grynkiewicz formula (Grynkiewicz et al., 1985) to fura-2 fluorescence recorded from 16 μm^2 zones. Running averages of $[Ca^{2+}]$ were performed before analysis using a window of five points. Images were collected with either a 20× (0.75 N.A.) objective or a 100× (1.3 N.A.) oil-immersion objective at 1 Hz. Fluctuations in fura-2 fluorescence were defined as spontaneous Ca^{2+} transients if they were greater than twice the noise level of baseline fluorescence (~3 nM peak to peak when measured with the 100× objective). Superfusion was continuous and the rate of perfusion was variable between 0.45 and 1.29 ml/min for the chamber volume of ~0.15 ml.

Electrophysiology. Whole-cell patch recordings from giant neurons in culture have been described previously (Saito and Wu, 1991; Zhao et al., 1995; Zhao and Wu, 1997; Yao and Wu, 1999; Peng and Wu, 2007a,b). Recording electrodes were pulled from glass capillaries to obtain a tip opening of ~1 μm and 3–5 MΩ input resistance in the bath. Normal pipette solution contained (in mM) 144 KCl, 1 $MgCl_2$, 0.5 $CaCl_2$, and 5

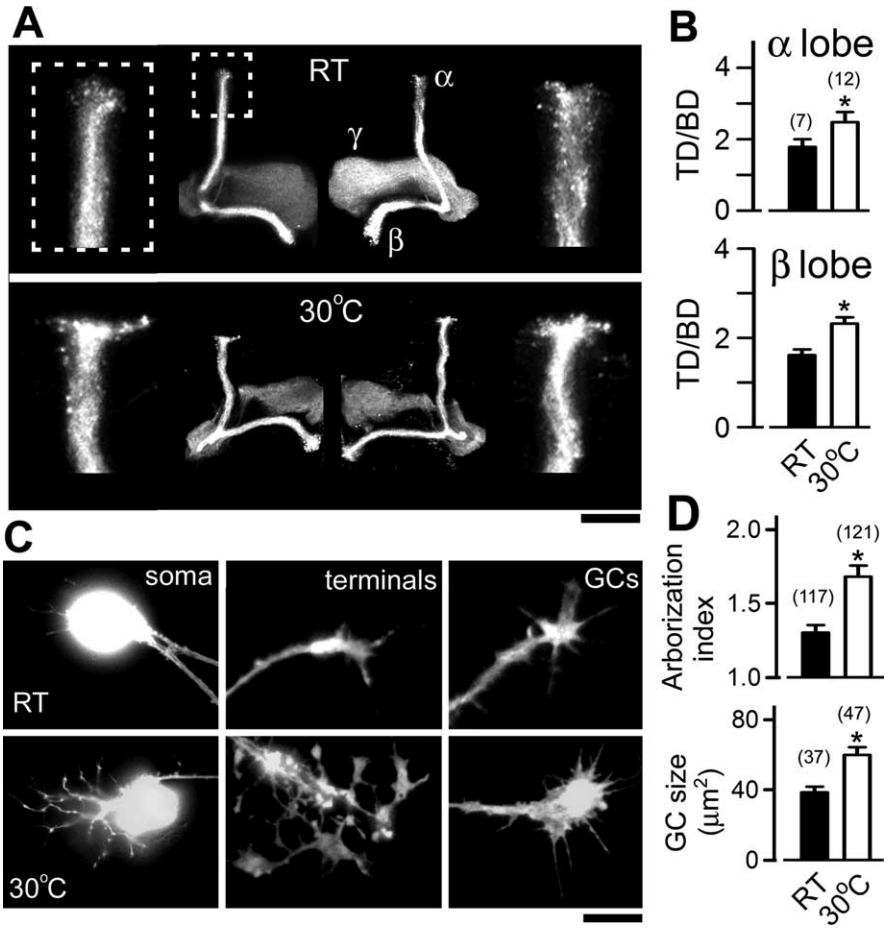

Figure 1. Enhanced neuronal growth *in vivo* and in culture by an increase in environmental temperature. ***A***, Confocal stack images of MB structures from 7-d-old WT male flies. Sibling flies were collected 1 d after eclosion and raised at RT (22–23°C) or 30°C for another 6 d. The GFP-labeled fluorescence was driven by the 201Y-Gal4 line. The left and right hemispheres are from different animals. MB lobes of α, β, and γ are marked as indicated. The terminal structures of the α lobes in the boxed area are enlarged four times in the inset. Note the increased terminal field arborization in 30°C-treated flies. Scale bar, 50 μm. ***B***, The extent of terminal arborization is indicated by the TD/BD ratio. The sample sizes are indicated in the parentheses. ***C***, Phase and fluorescent images of neurons labeled by 201Y-driven GFP expression cultured at RT and 30°C. Scale bar, 25 μm. ***D***, 201Y-labeled neurons displayed increased growth cone size and neurite terminal complexity (arborization index; see Materials and Methods) after an exposure to 30°C for 2 d. *$p < 0.05$, *t* test. Numbers in parentheses indicate cell numbers. Error bars indicate SEM. GC, Growth cone.

EGTA and was buffered at pH 7.1 with 10 HEPES. The bath solution was the same as for Ca^{2+} imaging. A patch-clamp amplifier (Axopatch 1B; Molecular Devices, Palo Alto, CA) and a computer in conjunction with an analog-to-digital (A/D)–D/A converter and pClamp software (version 5.5.1; Molecular Devices) were used to generate the current- and voltage-clamp commands and for data acquisition. For better isolation of Ca^{2+} currents, Ba^{2+} (20 mM) as well as Na^+ and K^+ channel blockers (10 nM TTX, 1 mM 4-AP, 2.5 mM TEA, and 0.05 mM quinidine) were added to the bath saline, and K^+ in the pipette solution was replaced by Cs^+ (Peng and Wu, 2007b). Voltage-activated K^+ currents were measured in the presence of Na^+ and Ca^{2+} channel blockers in the bath (10 nM TTX and 0.2 mM Cd^{2+}). Transient I_A and sustained I_K were determined with a 500 ms preconditioning pulse (to −20 mV from a holding potential of −80 mV), followed by a +60 mV test pulse 5 ms afterward (Zhao and Wu, 1997; Peng and Wu, 2007a).

Results

Kenyon cell terminal arborization *in vivo* and embryonic neuronal growth in culture are sensitive to developmental temperature

We first investigated how development at an increased temperature alters neuronal morphology within the *Drosophila* CNS. We used the GAL4-UAS system to visualize a subpopulation of MB Kenyon cells within the adult brain. By expressing a membrane-bound form of GFP (mCD8-GFP) with the 201Y-GAL4 driver (Yang et al., 1995), the pattern of mCD8-GFP fluorescence revealed individual lobes (α, β, and γ) consisting of axon branches of Kenyon cells. This expression pattern was confirmed by immunostaining against the adhesion molecule fasciculin II (data not shown), which expresses intensely in the MB (Crittenden et al., 1998). With the aid of GFP fluorescence, we found that exposure to the high temperature (30°C) from days 2–7 after eclosion caused a striking increase in the diameter of Kenyon cell axon terminals (quantified as TD) compared with RT (22°C) controls. This was true for both the α and β lobes of male (Fig. 1*A*) and female flies (data not shown). However, there was no significant change in the diameter of axon bundles (BD). The ratio of the two diameters (TD/BD) demonstrated the degree of terminal field expansion at high temperature (Fig. 1*B*). These parameters, TD, BD, and TD/BD, did not change when control flies were reared at RT throughout the 7 d (data not shown). Therefore, our data suggest that the temperature experienced by the flies during early adulthood promotes the growth of MB Kenyon cell presynaptic terminal arbors.

To examine how neuronal morphology changes in response to high temperature independent of cell–cell interactions, we used the well characterized giant neuron culture system derived from *Drosophila* embryonic neuroblasts (see Materials and Methods). In cultures made from single embryos, the 201Y-GAL4 line labels a discrete and relatively small population of neurons (Berke and Wu, 2002; Peng and Wu, 2007a). High-magnification images highlighted a pronounced increase in neurite terminal branching after exposure to high temperature for 2 d (Fig. 1*C*,*D*). An arborization index based on the weighted average of individual arbor types (see Materials and Methods and Figs. 2 and 3) provided a quantitative measure of arborization complexity. Notably, high temperature induced excessive neurite projections directly from the soma, although there was no obvious effect on the size of the cell body (Fig. 1*C*). Interestingly, the neuronal growth cone, known for sensing target cells during synapse formation, became ~50% larger in 201Y-positive cells when cultures were exposed to 30°C for 2 d (Fig. 1*C*,*D*). Therefore, high temperature induced an overgrowth of nerve terminals both *in vivo* and in culture, although the cells were grown under different environments and observed at different developmental stages.

Giant neuron cultures consist of heterogeneous cell populations differentiated from different neuroblast lineages (see Materials and Methods), and, in fact, temperature-induced morphological changes were common to a variety of these neuronal types. A majority of cells grown at 30°C displayed more complex ar-

borization accompanied by enlarged growth cones (Fig. 2*A*,*B*). Representative nerve terminal arbors of individual categories are depicted in Figure 2*C*, with the population distribution among the corresponding categories provided in Figure 3*A*. Development at high temperature had a strong effect on arborization among all neuronal types, including monopolar, bipolar, and multipolar cells (Fig. 3*B*). Importantly, exposure to 30°C for only 1 d [i.e., 2 d *in vitro* (DIV); see Materials and Methods] was sufficient to enhance arborization in these growing cells, with the effect plateauing by 3 DIV (Fig. 3*C*). The excessive branching was also characterized by an increase in the total length of the arbor per primary neurite and the average arbor length per internode segment (data not shown). A strong influence of temperature on growth cone morphology was also indicated by a higher percentage of monopolar, bipolar, and multipolar cells displaying large, expanded growth cones (Figs. 2*A*,*B*, 3*D*,*E*). The enlarged growth cones became evident after 1 d at high temperature (i.e., 2 DIV), reaching a maximum after 3 DIV, and paralleled the time course of increased arborization complexity (Fig. 3*C*,*F*). It is not known why terminal overbranching and growth cone enlargement do not increase further after 3 DIV and whether additional growth may be induced if high temperature is experienced beyond 6 DIV.

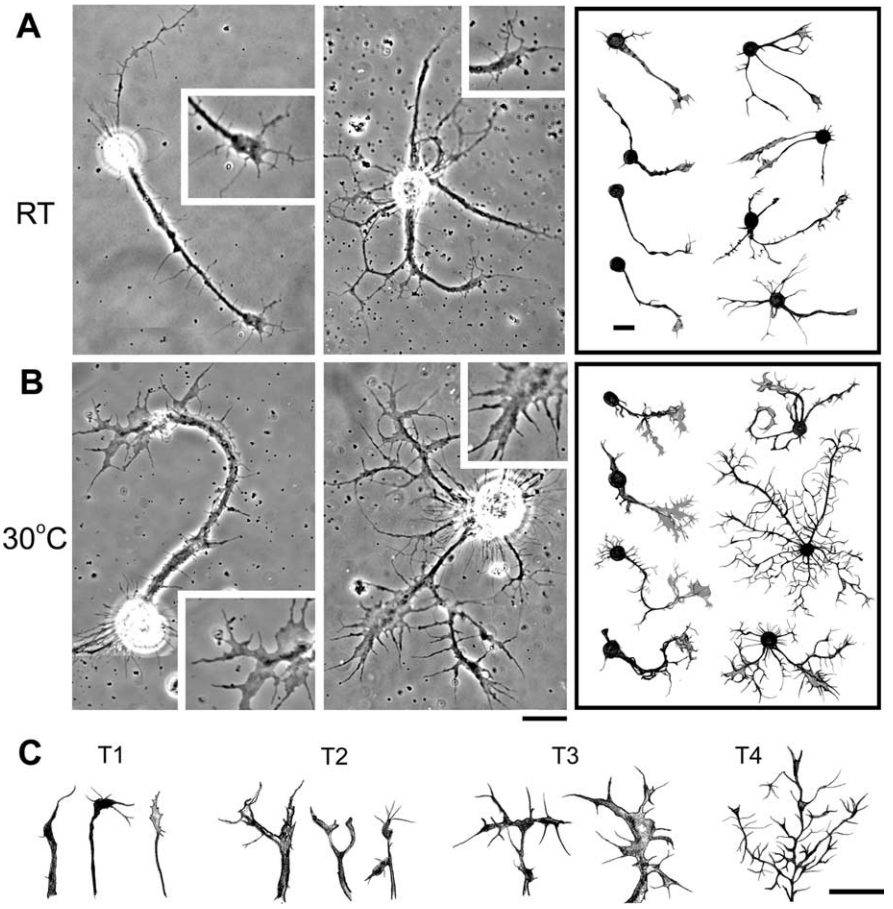

Figure 2. Examples of the temperature-induced increase in growth cone size and terminal arborization. Phase images of giant neurons cultured at different temperatures are shown. ***A***, ***B***, Cultures were initially grown at RT for 1 d and another 2 d at either RT (***A***) or 30°C (***B***). Insets show the growth cones enlarged 1.5 times. In the right panels, hand-drawn examples of monopolar, bipolar, and multipolar cells demonstrate enlarged growth cones and highly ramified neurites after a 2 d exposure to 30°C. ***C***, Hand-drawn examples of neurite terminals from different neurons. The terminals were classified into four types based on geometric complexity: T4 > T3 > T2 > T1 (see Materials and Methods). Scale bars, 20 μm.

We examined intracellular cytoskeleton organization by using the Gal4-UAS expression system after high-temperature treatment. As shown previously in *Drosophila* neuronal cultures and in other preparations, the established terminal branches contain both actin and microtubule cytoskeletons, whereas the mobile filopodia and flattened lamellipodia edges are supported by actin filaments only. Microtubule assembly, indicated by the GFP signal of α-tubulin ($elav^{C155}$-Gal4/+; UAS-GFP-α-tub/+; see Materials and Methods) was seen in the central domain of growth cones but was also profusely expressed in the complex arbor of neurons grown at 30°C (Fig. 4*A*). Actin filaments, visualized by the GFP signal of the filamentous actin-binding protein GMA ($elav^{C155}$-Gal4/UAS-GMA; see Materials and Methods), were observed in the edge of growth cones and in filopodia, in particular in the profuse filopodial decorations along neurites and growth cones grown at 30°C (Fig. 4*B*). However, actin but not tubulin was present within some of the higher-order fine branches of complex arbors, indicating their filopodial identity. Similar conclusions have been reached using a tubulin antibody and phalloidin to label the microtubule and actin cytoskeletons, respectively (data not shown).

High temperature enhances membrane excitability and spontaneous Ca^{2+} dynamics

Previous studies have shown that high-temperature rearing and hyperexcitability K^+ channel mutations both produce an increase in nerve terminal arborization at *Drosophila* peripheral neuromuscular junctions (Budnik et al., 1990; Sigrist et al., 2003; Zhong and Wu, 2004). High temperature might therefore lead to morphological modifications through specific neuronal physiological mechanisms, including alterations to membrane excitability. We investigated this possibility by examining electrical activity and Ca^{2+} dynamics in different subcellular regions of individual neurons in temperature-treated giant neuron cultures.

Activity-dependent accumulation of intracellular Ca^{2+} regulates both growth cone morphology and nerve arborization. If exposure to high temperature increases excitability, intracellular Ca^{2+} may be affected by an increased influx through voltage-gated Ca^{2+} channels. Fura-2 based Ca^{2+} imaging confirmed that high temperature greatly increased the proportion of cells with spontaneous Ca^{2+} transients (see responses before 250 s in Fig. 5*A*,*B*) (RT 7%, $n = 69$; 30°C 27%, $n = 74$). This activity was suppressed by both acute (100 nM; $n = 2$) and chronic (10 nM; $n = 13$) application of the Na^+ channel blocker TTX, suggesting an increase in membrane excitability as a source for promoting the spontaneous Ca^{2+} transients. Interestingly, a relatively mild depolarization caused by increasing extracellular K^+ from 2 to 4 mM preferentially affected high temperature-treated cultures, turning quiescent neurons into active ones (see traces and images between 250 and 350 s in Fig. 5*A*,*B*) (percentage of cells responding to 4 mM stimulation: RT, 0%; 30°C, ~10%). Importantly,

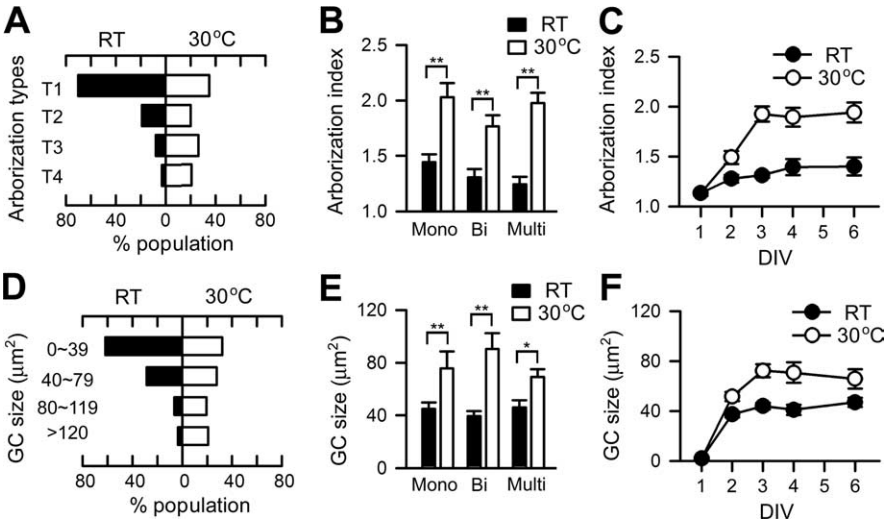

Figure 3. Quantification of temperature-dependent growth in culture. ***A***, Histogram of arborization types showing that the high-temperature condition induces more complex terminal arbors ($n = 485$) than RT ($n = 524$). ***B***, Arborization index based on the average of weighted sums of individual arborization types (see Materials and Methods), which indicates the extent of terminal arborization complexity. The temperature-induced arborization is observed in monopolar, bipolar, and multipolar neurons. $n =$ 125, 177, and 222 for RT; $n = 121$, 150, and 214 for 30°C. $^{**}p < 0.01$, *t* test. ***C***, Arborization indices of neurons cultured at RT or 30°C for different DIV. $n = 128$, 163, 524, 51, and 81 for 1–6 DIV at RT; $n = 128$, 133, 485, 74, and 71 for 30°C. ***D***, Histogram of growth cone size from neurons cultured at RT or 30°C ($n = 175$, 154). ***E***, The high temperature-induced growth cone enlargement is observed in monopolar, bipolar, and multipolar cells. $n = 49$, 60, and 66 for RT; $n = 40$, 52, and 62 for 30°C. $^{**}p < 0.01$; $^{*}p <$ 0.05 (*t* test). ***F***, The GC sizes observed in cultures grown at RT or 30°C for different DIV. $n = 28$, 89, 175, 46, and 42 for 1–6 DIV at RT; $n = 28$, 71, 154, 40, and 34 for 30°C. Error bars indicate SEM. Mono, Monopolar; Bi, bipolar; Multi, multipolar; GC, growth cone.

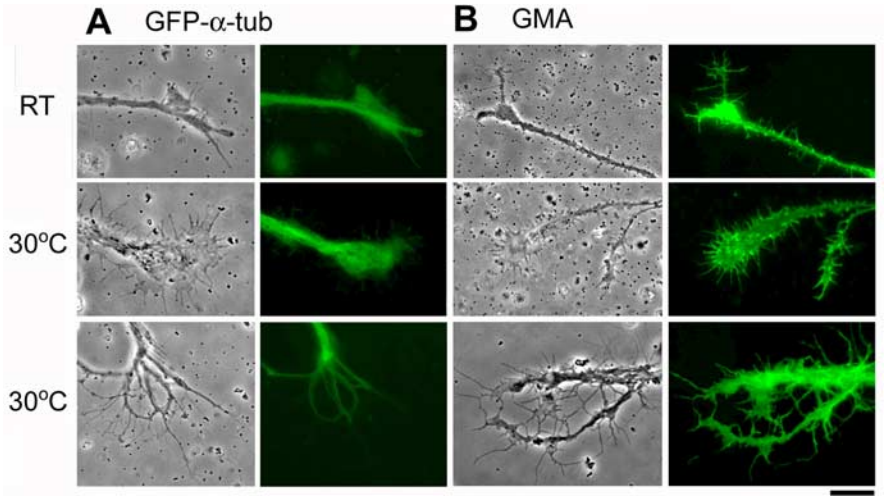

Figure 4. Cytoskeletal structures of the neurite terminals. ***A***, Phase and fluorescent images of neurite terminals in cultured neurons expressing GFP-tagged α-tubulin (GFP-α-tub) driven by pan-neural elav^{C155}-GAL4. The difference of the contours between phase and fluorescent images demonstrate that microtubules do not invade the peripheral area of expanded lamellipodia and high-order branches (fine protrusions) induced by high temperature. ***B***, Patterns of actin filaments revealed by GFP-tagged actin-binding domain of moesin (GMA) construct. In contrast, actin filaments are enriched in the lamellipodia and filopodia of the growth cone and fine high-order branches. Scale bar, 20 μm.

both the spontaneous and 4 mM K^+-induced Ca^{2+} dynamics were larger within the growth cone than within the soma (Fig. 5*B*) (cf. Berke et al., 2006).

Using whole-cell patch-clamp recording, we found evidence that high temperature increased neurite excitability and modified ion current expression. In RT cultures, ~45% of neurons displayed all-or-none action potentials (cf. Peng and Wu, 2007a), with regular trains of full-blown, overshooting spikes as recorded from the soma during injection of depolarizing current (Fig. 6*A*) (cf. Zhao and Wu, 1997; Yao and Wu, 1999). In contrast, cultures grown at 30°C had a higher percentage of spiking neurons [RT, 45% ($n = 158$); 30°C, 63% ($n =$ 48); $p < 0.05$, χ^2 test]. These spiking cells, often equipped with enlarged growth cones and complex terminal arbors, tended to display broadened but nonovershooting action potentials (Fig. 6*A–C*). During progressively increasing levels of step current injection, most neurons raised at 30°C exhibited such spike activities riding on top of varying levels of passive depolarization (data not shown). In contrast, the peak of the overshooting, full-blown action potentials in RT control cells was limited by a reversal potential although the baseline of passive depolarization increased after greater current injection (data not shown). In addition, temperature increased the population of cells with a prolonged delay in spike initiation [onset time, >100 ms; RT, 25%, ($n = 71$); 30°C, 70% ($n = 30$); $p < 0.001$]. More importantly, some of the nonovershooting spiking events in temperature-treated cultures appeared as doublets or triplets (RT, 0%; 30°C, 17%; $p < 0.01$) (Fig. 6*A*), indicating multiple spike initiation sites. These observations support the idea that full-blown local soma action potentials were replaced by signals propagating from remote initiation sites in the neurites, suggesting that high temperature enhances excitability in the well extended distal arbors. Another striking feature of the unusual regenerative potentials in 30°C-treated cultures was represented by irregular plateau potentials that showed a prolonged depolarization and failed to repolarize during current injection. Such cells were rarely seen in cultures grown at RT (RT, 1%; 30°C, 13%; $p < 0.05$) (Fig. 6*A*). These plateau potentials did have a clear reversal potential (data not shown) and may be an extreme case of spike broadening (Fig. 6*A*, *C*).

Given the altered spike activities, we investigated whether development at high temperature induced an altered composition of the underlying ion currents. Several types of currents were examined using ion substitution and pharmacological blockers during voltage-clamp recording. We first isolated the currents flowing through Ca^{2+} channels by adding K^+ and Na^+ channel blockers. Measurements of inward currents mediated by Ca^{2+} channels were further facilitated by using Ba^{2+} (20 mM) in the bath as the charger carrier (see Materials and Methods). Inward currents peaked approximately at 0 mV (Fig. 6*D*, *E*) (cf. Peng and Wu, 2007b). Strikingly, both the transient and sustained components of Ca^{2+} channel-mediated currents were upregulated in cultures grown at 30°C (Fig. 6*F*).

We also measured voltage-activated outward K^+ currents

(transient I_A and sustained I_K, isolated with prepulse voltage-clamp protocols) when inward Na^+ and Ca^{2+} channels as well as outward Ca^{2+}-activaterd K^+ channels were blocked (see Materials and Methods). Interestingly, in contrast to Ca^{2+} current upregulation, both I_A and I_K were downregulated in 30°C-treated cultures (Fig. 6*G*), presumably contributing to the observed membrane hyperexcitability. The increase in Ca^{2+} current density may explain the lengthening of action potentials and generation of plateau action potentials recorded at the soma during current injection. This effect may be further enhanced by weakened repolarization attributable to decreased K^+ currents (Fig. 6*A*,*C*). Our data therefore establish a correlation between the physiological and morphological alterations observed in isolated, growing neurons in response to an increase in environmental temperature.

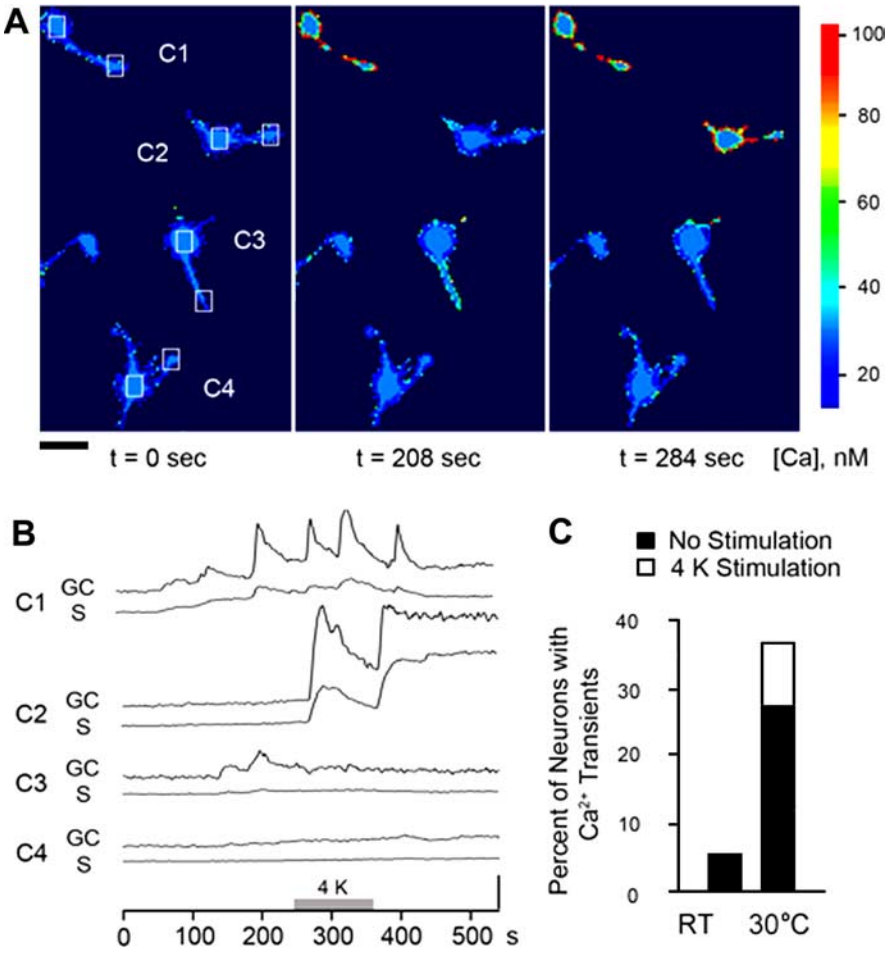

Figure 5. Increased spontaneous Ca^{2+} dynamics in cultures developed at high temperature. ***A***, A series of pseudocolor images of fura-2-loaded neurons in a 30°C-treated culture collected at indicated time points. The pseudocolor scale bar indicates estimated intracellular Ca^{2+} levels based on ratiometric fluorescence measurements. Scale bar, 25 μm. ***B***, The Ca^{2+} dynamics of the boxed areas in several cells (C1–C4) in ***A*** is quantified before, during, and after a 2 min exposure to 4 mM K^+ saline (4 K). GC, Growth cone; S, soma. Spontaneous activity was observed in cells C1 and C3 before the 4 mM K^+ stimulus. Note the consistently larger spontaneous events in the growth cone than in the soma and the 4 K-induced robust Ca^{2+} dynamics in cell C2. The vertical bar indicates 5 nM. ***C***, The percentage of neurons with spontaneous transients (filled portion) and the percentage of quiescent neurons that became active after perfusion of 4 mM K^+ (4 K; open portion). Cultures grown at 30°C tended to have a greater percentage of cells with spontaneous or 4 K-sensitive activities than cultures grown at RT. $n = 69$ for RT and 74 for 30°C.

Genetic and pharmacological analyses confirm the roles of hyperexcitability and Ca^{2+} influx in temperature-dependent developmental plasticity

We obtained additional lines of evidence to support a role for membrane hyperexcitability in high temperature-induced overgrowth by using drugs and mutants. In parallel to its suppressing effect on spontaneous Ca^{2+} dynamics described above, chronic application of TTX suppressed the morphological changes observed in temperature-treated WT cultures (Fig. 7). Furthermore, hyperexcitability attributable to *eag* and *Sh* K^+ channel mutations led to enhanced terminal arborization and enlarged the neuronal growth cones, even at RT (Fig. 7) (cf. Berke et al., 2006). These growth phenotypes could be mimicked by chronic application of 4-AP (I_A blocker) to WT cultures. Moreover, the hyperexcitability-induced growth in *Sh* neurons was suppressed by TTX (Fig. 7*B*,*C*).

In addition, Ca^{2+} imaging revealed an increase in the frequency of neurons with spontaneous Ca^{2+} transients in *Sh*-, *eag*-, and 4-AP-treated WT cultures [at RT: WT, 6% ($n = 69$); *Sh*, 24% ($n = 116$); *eag*, 17% ($n = 23$); 4-AP, 19% ($n = 26$); at 30°C: WT, 28% ($n = 74$)] (cf. Berke et al., 2006). Interestingly, *eag Sh* double-mutant neurons did not show a further enhancement of spontaneous Ca^{2+} transients (20%, $n = 10$) compared with neurons of either single mutant. Similarly, no further enhancement in the morphological changes was observed in *eag Sh* cultures (Fig. 7*B*,*C*). In the same vein, *Sh* and *eag* single-mutant neurons cultured at 30°C failed to grow beyond the levels of their RT controls (Fig. 7*B*,*C*). It is worth noting that cultured neurons related to the Kenyon cell lineages identified by the 201Y-Gal4 driver also displayed robust spontaneous Ca^{2+} dynamics and increased terminal outgrowth induced either by an *eag* mutation or 4-AP-treatment on WT cultures (see Fig. 10).

Because neuronal activity facilitates Ca^{2+} influx through voltage-gated Ca^{2+} channels to influence intracellular Ca^{2+} dynamics, we examined the effects of a Ca^{2+} channel mutation, *cac*, that greatly reduces Ca^{2+} currents in cultured giant neurons (Peng and Wu, 2007b) and depolarization-induced Ca^{2+} transients (data not shown). The *cac* mutation by itself did not alter growth cone sizes and arborization indices but blocked the ability of high temperature to increase these morphological indicators (Fig. 7*B*,*C*). The results suggest a role for Cac channels in mediating Ca^{2+} influx during temperature-dependent neuronal growth.

In vivo roles of hyperexcitability and cAMP signaling in MB development

The conclusions derived from mutant cultures (Fig. 7) were also applicable to MB Kenyon cell growth *in vivo*. With the same 201Y-GAL4 driver and UAS-mCD8-GFP responder (compare Fig. 1), we visualized MB arbors in different hyperexcitable mutant backgrounds. In *eag*, *Sh*, or *eag Sh* mutant animals raised at RT, the terminal arbors of both α and β lobes were expanded, similar to, or even larger than, the expansion produced by development at 30°C in WT adults (Fig. 8*A*,*B*, TD/BD). Notably, *eag*

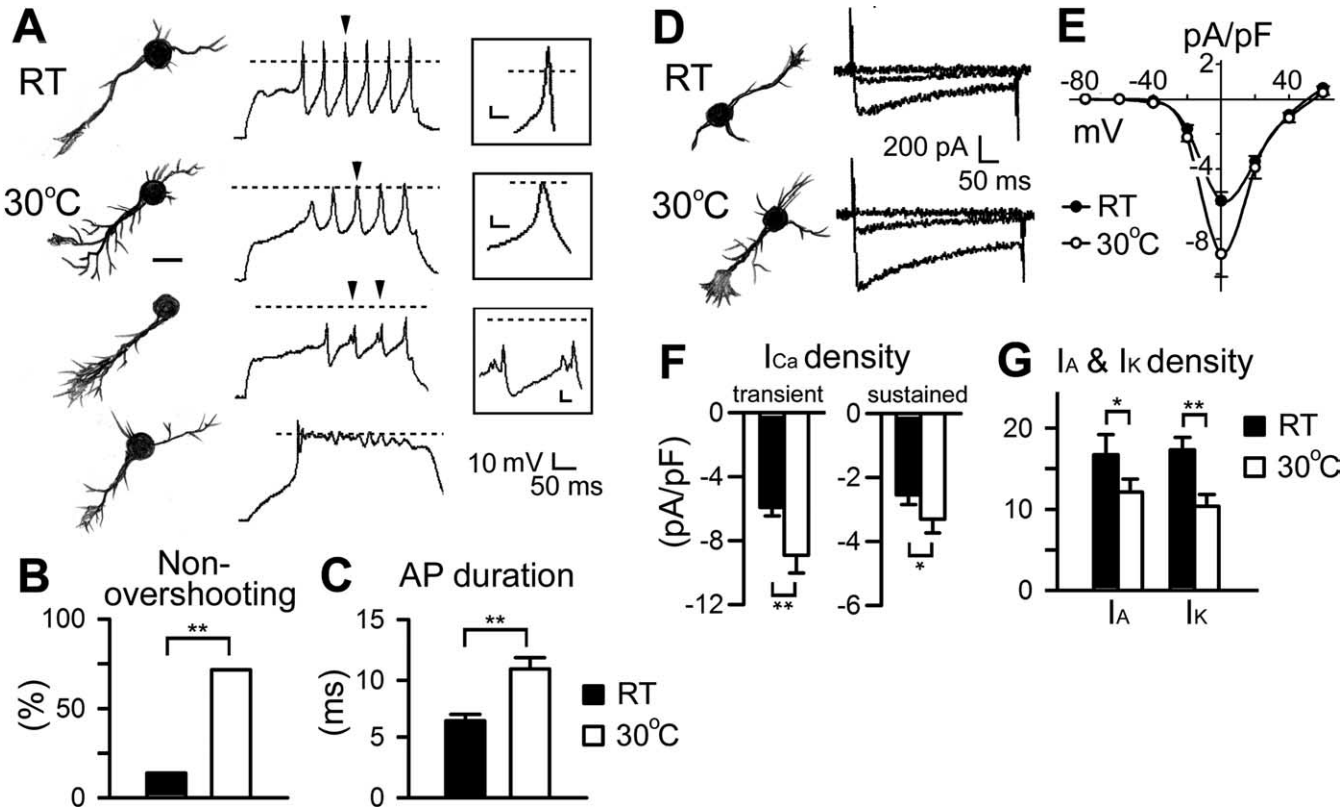

Figure 6. Changes in action potential firing and ion currents in high temperature-treated cultures. ***A***, Hand drawings of representative neurons cultured at RT and 30°C and the corresponding firing patterns obtained during current-clamp recordings. Unlike the typical regular firing patterns displayed by neurons in RT cultures (top panels), neurons in 30°C cultures (bottom panels) frequently generated nonovershooting spikes, spikes with multiple peaks, and plateau potentials. Scale bar, 25 μm. Dashed lines indicate 0 mV. Insets, Enlarged action potentials that are labeled by arrowheads. Calibration: 5 mV, 10 ms. ***B***, Percentage of neurons with nonovershooting spikes at different temperature. $n = 71$ for RT and 30 for 30°C. $^{**}p < 0.01$, χ^2 test. ***C***, Action potential (AP) durations obtained from neurons grown at different temperatures. ***D***, Examples of neuronal morphology and corresponding Ca^{2+} channel-mediated currents in voltage-clamp condition. Superimposed traces represent responses to test pulses from −80 to 0 and +20 mV. The saline contained 20 mM Ba^{2+}, 1.8 mM Ca^{2+}, as well as blockers for K^+ and Na^+ channels. Cs^+ replaced K^+ in the pipette solution. ***E***, *I–V* curves of peak Ca^{2+} channel-mediated currents from neurons cultured at different temperatures. The density (in pA/pF) of inward currents peaked approximately at 0 mV. $n = 117$ for RT and 32 for 30°C. ***F***, Greater current densities of the transient (peak) and sustained (steady-state) components at 0 mV in neurons cultured at 30°C than that in non-temperature-treated neurons. ***G***, Decreased voltage-activated transient I_A and sustained I_K in neurons raised at high temperatures. I_A and I_K were isolated by a prepulse conditioning protocol with the presence of Na^+ and Ca^{2+} channel blockers (see Materials and Methods). $n = 30$ for RT and 30 for 30°C. Error bars indicate SEM. $^*p < 0.05$; $^{**}p < 0.01$ (*t* test).

Sh double-mutant flies did not produce significantly greater terminal expansion than either single mutant alone.

Our culture data indicate an important role for depolarization-induced Ca^{2+} influx, which is known to trigger several second-messenger pathways, including the cAMP cascade. cAMP signaling regulates activity-dependent neuronal plasticity, including the modulation of motoneuron growth by temperature and K^+ channel mutations (Zhong et al., 1992; Zhong and Wu, 1993; Renger et al., 2000). With the *dnc* and *rut* mutations, which affect a cAMP-dependent PDE and a Ca^{2+}/calmodulin-dependent AC (Byers et al., 1981; Livingstone et al., 1984; Tully and Quinn, 1985), we found that cAMP also regulates temperature-dependent neuronal growth within the CNS. Kenyon cell arbors in rut^2 flies were not different from those of WT control, whereas dnc^1 increased terminal arborization (Fig. 8*A*,*B*).

cAMP signaling in cell-autonomous regulation of neuronal growth was investigated in giant neuron cultures. The effects of hyperexcitability induced by high temperature, K^+ channel mutations, or pharmacological blockers were studied in a *rut* mutant background. The most striking *rut* effect was the suppression of overgrowth caused by hyperexcitability. Both growth cone size and arborization index were no longer different from WT controls in rut^1 Sh^M double-mutant cultures or in 4-AP-treated *rut* cultures (Fig. 9*B*,*C*). Mutations of *rut* also suppressed some aspects of temperature-induced neuronal growth. We observed in rut^1 but not rut^2 cultures a small increase in growth cone size and arborization index (Fig. 9*B*,*C*). However, rut^1 neurons did not display the increase in arborization index when grown at high temperature (Fig. 9*C*). Notably, neither allele of *rut* prevented the growth cone enlargement after high temperature treatment (Fig. 9*B*). These observations indicate that the signaling processes that may be downstream of Ca^{2+} in temperature-induced growth may not be identical with respect to growth cone expansion and neurite branching.

To establish an independent line of evidence in support of the critical role of the Rut AC, a rescue experiment was performed by expressing UAS-rut+ (Liu et al., 2006) using the 201Y-Gal4 driver in a *rut* mutant background. Giant neuron cultures prepared from rut^1/rut^1; 201Y-Gal4, UAS-GFP/UAS-rut+ embryos were subjected to high-temperature treatment. Among 201Y-positive neurons, targeted expression of UAS-Rut+ reverted the suppression effect of the rut^1 mutation on the temperature-induced terminal overbranching (Fig. 10). This observation further delineates the role of the Rut adenylyl cyclase in different aspects of temperature-induced neuronal growth (i.e., terminal arborization vs growth cone expansion).

Discussion

This study presents a common theme by which temperature promotes nerve terminal outgrowth for neurons in both the central and peripheral nervous systems, as well as for cultured neurons devoid of cell–cell contacts. Direct monitoring by optical imaging and electrophysiological recording from cultured neurons corroborated the genetic and pharmacological evidence that high temperature enhances membrane excitability levels through ion channel regulation and that the interplay of K^+ and Ca^{2+} channels leads to increased cytosolic Ca^{2+} levels. Activation of the Ca^{2+}-dependent Rut AC in turn triggers the cAMP-dependent pathway to regulate this striking developmental plasticity (Fig. 11).

Environmental temperature and axonal terminal outgrowth *in vivo*

Quantitative measurements of the larval neuromuscular junction have demonstrated that high temperature promotes the growth of peripheral nerve branches and synapses (Sigrist et al., 2003; Zhong and Wu, 2004). The current study extends this observation to the MB (Figs. 1, 8), a developmentally well characterized CNS structure (Ito et al., 1997; Lee et al., 1999) important for learning and memory (Heisenberg, 1998). Whereas postsynaptic expression of muscle glutamate receptors has been implicated in the temperature-dependent synaptic overgrowth at larval neuromuscular junctions (Sigrist et al., 2003), presynaptic nerve excitability also plays a definitive role, as indicated by the suppression of such overgrowth by Na^+ channel mutations (Sigrist et al., 2003; Zhong and Wu, 2004). It is known that Na^+ channels express in neurons but not muscle cells, which rely on Ca^{2+} channels for depolarization (Singh and Wu, 1999). Our study on dissociated cultures confirms that enhanced membrane excitability is responsible for the temperature-dependent growth of single neurons, even without interactions between presynaptic and postsynaptic elements.

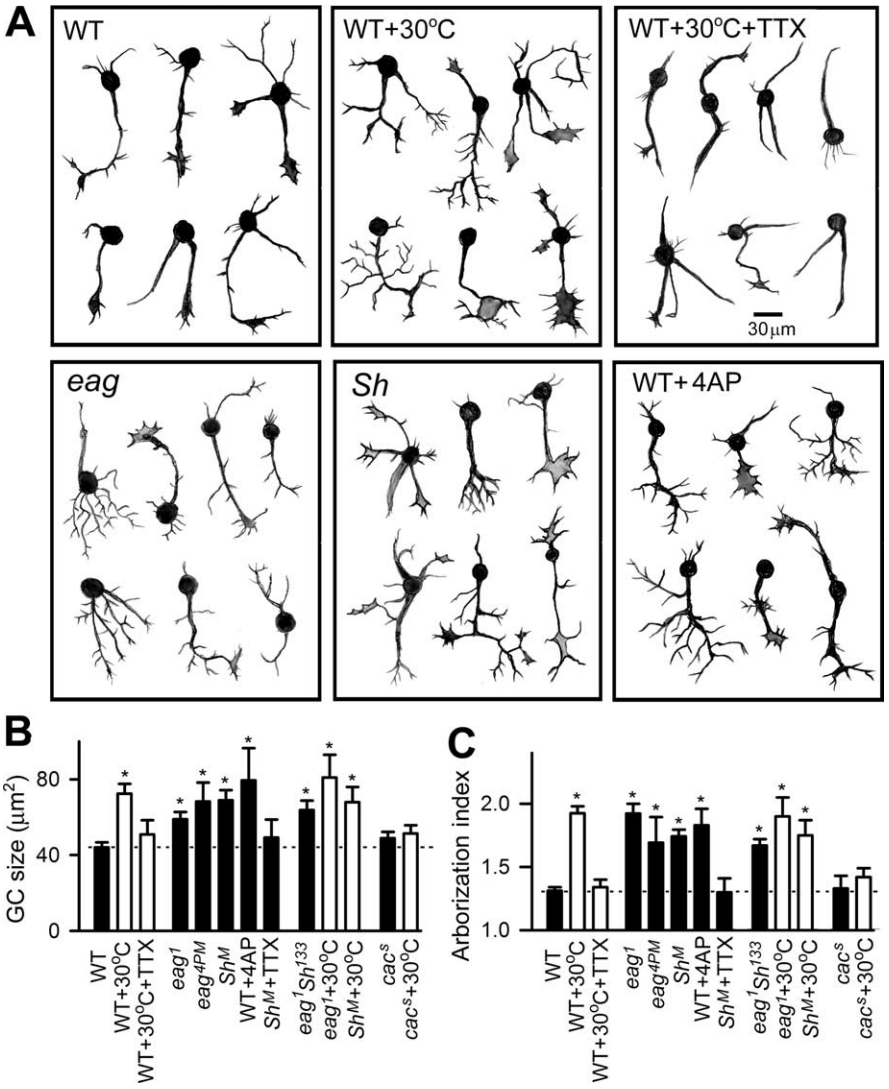

Figure 7. Similar neuronal overgrowth induced by membrane hyperexcitability and high-temperature treatment. ***A***, Hand drawings of WT neurons treated with Na^+ and K^+ channel blockers (TTX and 4-AP, respectively) and neurons of different K^+ channel mutants. The high temperature-induced neurite terminal outgrowth could be suppressed by chronic treatment of TTX (1 μM). Cultured *eag* and *Sh* neurons as well as 4-AP-treated WT neurons displayed increases in growth cone size and neurite terminal branching. ***B***, ***C***, The averaged growth cone (GC) size and arborization index from individual genotypes or experimental conditions. Cultures of *eag Sh* double mutants at RT and cultures of corresponding single mutants raised at 30°C (*eag*+30°C and *Sh*+30°C) displayed an increase in neurite terminal growth compared with that in WT cultures at RT, but not significantly greater than the corresponding single-mutant effects at RT. Furthermore, a mutation of a Ca^{2+} channel, cac^s, suppressed high temperature-induced terminal overgrowth. $n \geq 30$ for growth cone size and ≥ 60 for arborization index. Error bars indicate SEM. $^*p < 0.05$, one-way ANOVA against WT at RT.

Postsynaptic RNA regulation and protein synthesis conceivably contribute to temperature-dependent synaptic overgrowth *in vivo*, as indicated by the mutational effects of the poly(A)-binding protein gene in muscle at an elevated temperature (Sigrist et al., 2003). Release of retrograde signals by postsynaptic partners (Petersen et al., 1997; Haghighi et al., 2003; McCabe et al., 2003) may also occur during temperature-induced synaptic growth *in vivo*, a possibility that is indicated by the effects of postsynaptic Ca^{2+} and Ca^{2+}/calmodulin-dependent kinase II (CaMKII) on neurotransmission at embryonic neuromuscular junctions (Kazama et al., 2003, 2007; Yoshihara et al., 2005). However, our study using dissociated embryonic cultures demonstrates that isolated neurons devoid of cell–cell contacts are capable of striking temperature-induced neurite outgrowth. This cell-autonomous mechanism may be responsible for the initial growth after a temperature increase, whereas interactions between synaptic partners can, in principle, modulate synaptic growth and maintain functional connections.

Interplay of K^+ and Ca^{2+} channels regulating developmental plasticity induced by high temperature

Our results from cultured neurons indicate that the modulation of K^+ and Ca^{2+} channels by high temperature increases membrane excitability, leading to enhanced Ca^{2+} dynamics especially within the growth cone and eventually to neurite outgrowth. First, there was a striking parallel in nerve terminal overgrowth between cultures of hyperexcitable K^+ channel mutants (*eag*, *Sh*,

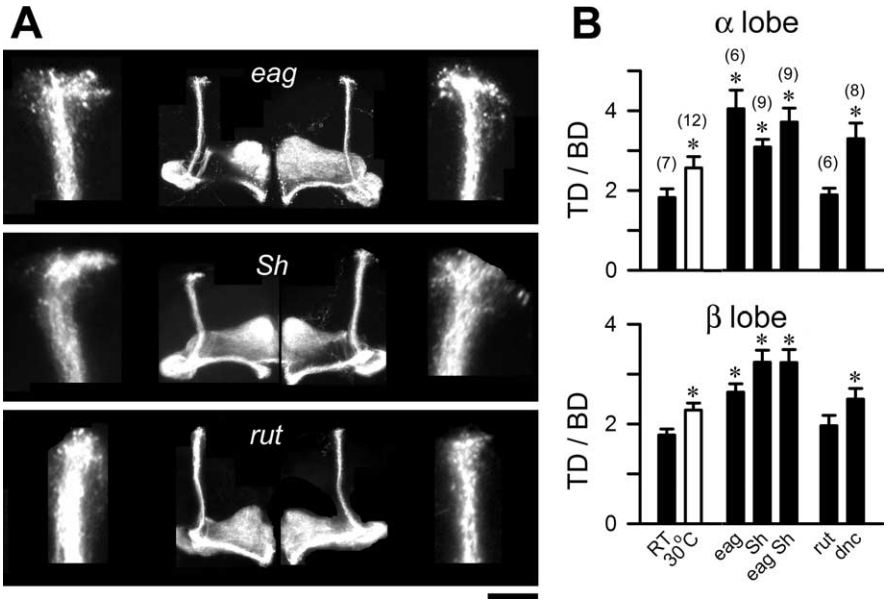

Figure 8. Mutational analyses of MB Kenyon cell growth at RT *in vivo*. ***A***, MBs from 7-d-old male flies raised at RT in different genetic backgrounds that expressed UAS-CD8-GFP driven by 201Y-GAL4 (see Fig. 1 for details). Scale bar, 50 μm. ***B***, The TD/BD ratios indicate that all K^+ channel (*eag*, *Sh*, and *eag Sh*) and *dnc* mutations, but not *rut*, resulted in an increase of terminal arborization in both α and β lobes. The sample sizes are indicated in the parentheses. $*p < 0.05$, one-way ANOVA. Error bars indicate SEM.

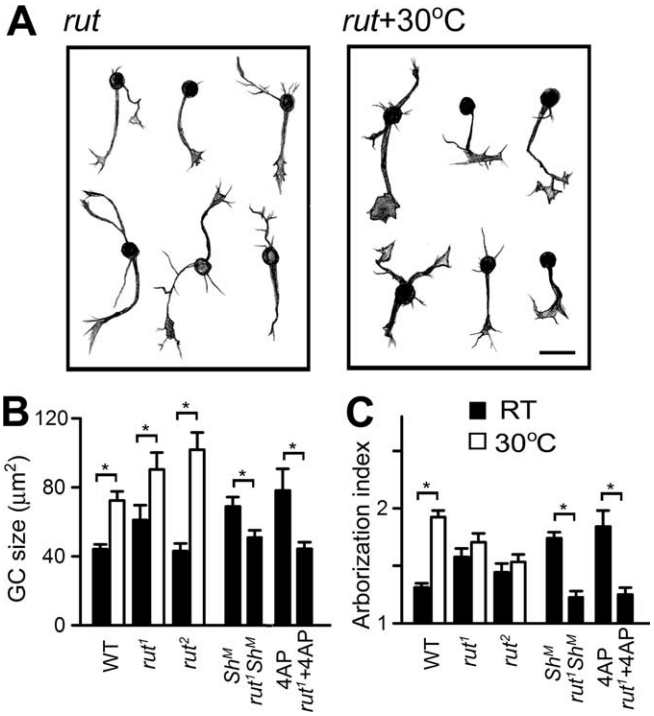

Figure 9. Involvement of the cAMP pathway in temperature- and K^+ channel blockade-induced overgrowth in cultured neurons. ***A***, Hand drawings of neurons from *rut* cultures grown at RT and 30°C. Scale bar, 25 μM. ***B***, ***C***, The averaged growth cone (GC) size and arborization index for individual genotypes and experimental conditions. Note that mutations of *rut* suppressed the temperature-, *Sh*-, or 4-AP-induced arborization (***C***), whereas the temperature-induced enlargement of growth cones was not blocked by *rut* (***B***). Error bars indicate SEM. $n \geq 30$ for GC size and ≥ 60 for arborization index.

and *eag Sh*) at RT and WT cultures grown at high temperature (Figs. 2, 7). Such terminal overgrowth could also be mimicked in WT cultures by pharmacological blockade of K^+ currents (Fig. 7). Third, direct imaging revealed frequent spontaneous Ca^{2+} transients in WT cultures grown at high temperature and in K^+ channel mutant cultures at RT (Fig. 5). Fourth, when neuronal excitability was reduced by blocking Na^+ channels with TTX, the spontaneous Ca^{2+} transients, enlarged growth cones, and high-order terminal arbors induced by either high-temperature treatment or K^+ channel mutations disappeared (Figs. 5, 7). Finally, whole-cell recording of neurons reared at 30°C revealed an upregulation of Ca^{2+} currents, a downregulation of K^+ currents, and an increased population of neurons capable of firing all-or-none spikes or plateau potentials (Fig. 6) (see Results).

A higher excitability level in distal neurites and growth cones was reflected by the greater size of spontaneous Ca^{2+} transients in these distal regions, which occurred more frequently in 30°C-treated WT cultures (Fig. 5). Electrophysiological recording indicated a distal shift of the spike initiation site away from the soma, and a prevalence of doublets or triplets of spike activities (instead of single spikes) presumably reflects multiple action potential initiation sites in the complex arbors (Fig. 6). These excitability patterns have been described in the soma of neurons in semiintact preparations of *Drosophila* (Choi et al., 2004) and other invertebrates (Burrows, 1996) that display complex branching patterns. Therefore, these effects are not abnormal but, rather, may be a natural outcome of neuronal maturation.

Intracellular Ca^{2+} dynamics regulate neuronal development, including lamellipodial expansion, filopodial elongation, and growth cone motility (Gomez and Spitzer, 1999; Lau et al., 1999; Zheng, 2000) by cytoskeletal reorganization (Fields et al., 1990; Berke et al., 2006). Our study reveals the role of Ca^{2+} channels in the temperature-promoted neuronal growth. Mutations of the *cac* locus, encoding a voltage-gated Ca^{2+} channel, severely reduce neuronal Ca^{2+} currents (Peng and Wu, 2007b) and suppress temperature-induced neurite overbranching and growth cone enlargement (Fig. 7). However, our results do not rule out a role of Ca^{2+} release from intracellular Ca^{2+} stores in temperature-dependent growth, which needs further investigation.

It has been proposed that the accumulation of intracellular Ca^{2+} beyond a set point no longer promotes neuronal growth (Cohan et al., 1987). It is known that double-mutant *eag Sh* larvae display more extreme neuronal hyperexcitability than either single mutant at neuromuscular junctions (Wu et al., 1983; Gho and Ganetzky, 1992). Our results indicate that in both the adult CNS and embryonic cultures, *eag* and *Sh* mutants displayed terminal overgrowth at RT (22–23°C), but such growth was not further enhanced in *eag Sh* double mutants (Figs. 7, 8). Moreover, the extent of terminal overgrowth of these K^+ channel mutants was not further enhanced when grown at high temperature (Fig. 7). However, neuronal overgrowth at the larval neuromuscular junction is induced by a milder temperature increase and could be observed at 25°C in *eag* or *Sh* single mutants and at 18–21°C in double mutants (Zhong et al., 1992; Zhong and Wu, 2004).

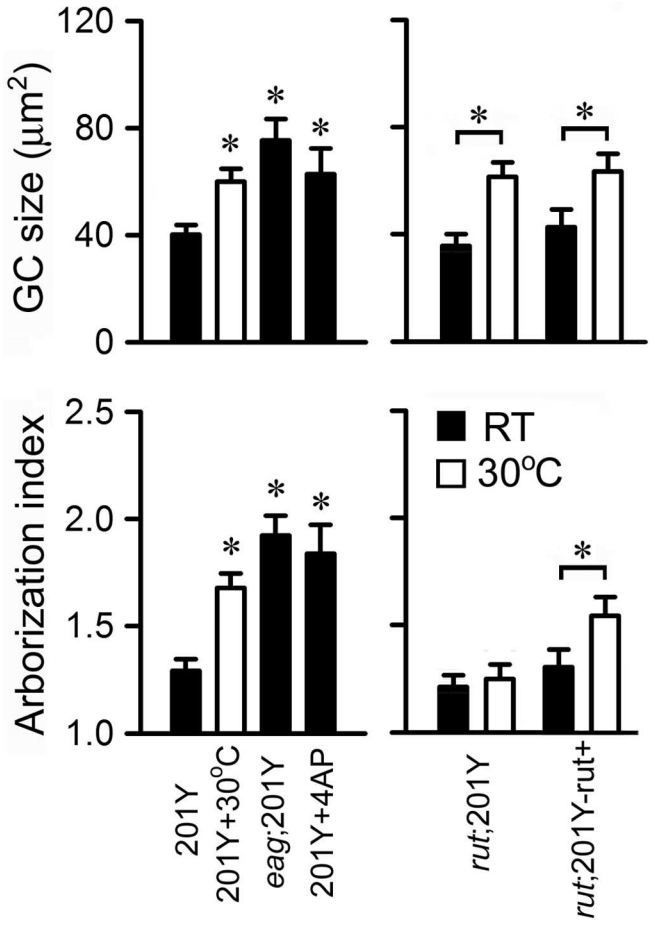

Figure 10. Morphological effects of hyperexcitability and the role of the Rut AC in temperature-induced growth of 201Y-positive neurons in giant neuron cultures. Either an *eag* mutation or the application of 4-AP to WT neurons significantly increased growth cone (GC) size and arborization index comparable to high temperature-induced growth enhancement, whereas the rut^1 mutation suppressed temperature-induced terminal overbranching but not growth cone enlargement. Expressing UAS-rut+ using the 201Y-Gal4 driver in a *rut* mutant background (rut^1/rut^1; 201Y-Gal4, UAS-GFP/UAS-rut+) reverted the suppression effect of rut^1 on the temperature-induced overbranching. Error bars indicate SEM. $n \geq 25$ for GC size and ≥ 50 for arborization index. $^*p < 0.05$, one-way ANOVA (left) or paired *t* test (right).

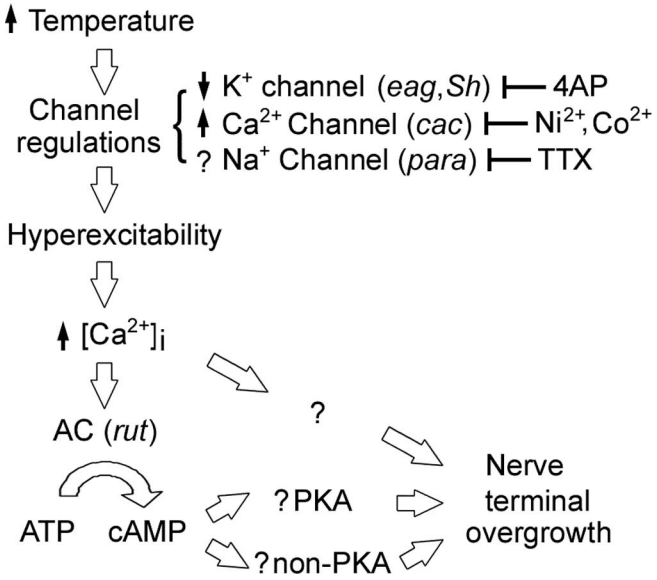

Figure 11. Summary of temperature-induced cellular events that mediate neuronal overgrowth. An increase in environmental temperature modulates several ion currents to increase membrane excitability. The interplay of K^+ and Ca^{2+} currents leads to increased cytosolic Ca^{2+} levels, resulting in activation of the Ca^{2+}-dependent Rut AC, which in turn triggers cAMP-dependent pathways to regulate the striking nerve terminal overgrowth. However, other molecular mechanisms are likely to also participate. PKA, Protein kinase A.

cAMP and temperature-induced overgrowth

It is worth noting that, when comparing the morphology of neurons in culture with neuronal structures *in vivo*, we contrast developing embryonic structures to the end results of postembryonic growth. Remarkably, the cAMP pathway exerts similar actions on nerve terminal branching both in cultured neurons deprived of cell–cell interactions (Fig. 9) and in intact adult CNS MB Kenyon cells (Fig. 8) and larval PNS neuromuscular junctions (Zhong and Wu, 2004) complete with postsynaptic targets. Disruptions in cAMP metabolism by *rut* mutations suppress the branch overgrowth induced by high temperature or K^+ channel blockade (Fig. 9, 30°C, Sh^M and 4-AP), which could be rescued by transgenic expression of *rut*+ (Fig. 10). In addition, increased cAMP levels in *dnc* mutant flies promoted overgrowth of axon terminals of MB Kenyon cells (Fig. 8) and larval motoneurons (Zhong et al., 1992).

The processes controlling growth cone development and motility determine neurite elongation and branching. Previous studies in cultured *Drosophila* neurons have demonstrated the involvement of cAMP in growth cone motility and Ca^{2+} regulation (Kim and Wu, 1996; Berke and Wu, 2002), possibly involving ion channel modulation, as has been shown for muscle and nerve K^+ channels (Zhong and Wu, 1993; Zhao and Wu, 1995). Growth cone morphology and neurite branching in culture were both affected by high-temperature and K^+ channel perturbations (Fig. 7). However, cAMP-dependent regulation appears to differentially mediate the effects of high temperature and hyperexcitability on growth cone size. In contrast to the case of branch overgrowth, *rut* mutations suppressed only K^+ channel- but not high temperature-induced growth cone expansion (Figs. 9, 10).

Downstream effectors of the cAMP pathway have been implicated in mediating synaptic growth to affect behavior such as learning. A downstream target of cAMP-dependent protein kinase, the transcription factor CREB (cAMP response element-binding protein) modulates activity-dependent synaptic growth in *Drosophila* (Davis et al., 1996) and *Aplysia* (Bailey and Kandel, 1993). Altered expression of the Fas II adhesion molecule is also required for synaptic overgrowth induced by *eag*, *Sh*, or *dnc* mutants (Schuster et al., 1996), suggesting that modulation of cellular adhesion may be an important mediator of temperature-dependent growth.

Other signal transduction pathways may also contribute to growth cone development and its regulation by high temperature. It is known that mutations of the CaMKII and cGMP-dependent protein kinase (PKG) pathways can severely modify axon terminal branching at the neuromuscular junction (Wang et al., 1994; Renger et al., 1999). Cultured neurons carrying variants of the PKG locus differ in spontaneous action potential activities and voltage-gated K^+ currents (Renger et al., 1999). Preliminary analysis in culture suggests that these variants differ with respect to spontaneous Ca^{2+} dynamics and growth cone morphology (data not shown). It will be interesting to dissect how these different signal transduction pathways act in concert or independently to mediate temperature-dependent neuronal growth.

References

Bailey CH, Kandel ER (1993) Structural changes accompanying memory storage. Annu Rev Physiol 55:397–426.

Berke B, Wu CF (2002) Regional calcium regulation within cultured *Drosophila* neurons: effects of altered cAMP metabolism by the learning mutations dunce and rutabaga. J Neurosci 22:4437–4447.

Berke B, Lee J, Peng I-F, Wu CF (2006) Sub-cellular Ca2+ dynamics affected by voltage- and Ca2+-gated K+ channels: regulation of the soma-growth Cone disparity and the quiescent state in *Drosophila* neurons. Neuroscience 142:629–644.

Bloor JW, Kiehart DP (2001) zipper Nonmuscle myosin-II functions downstream of PS2 integrin in *Drosophila* myogenesis and is necessary for myofibril formation. Dev Biol 239:215–228.

Brand AH, Perrimon N (1993) Targeted gene expression as a means of altering cell fates and generating dominant phenotypes. Development 118:401–415.

Budnik V, Zhong Y, Wu CF (1990) Morphological plasticity of motor axons in *Drosophila* mutants with altered excitability. J Neurosci 10:3754–3768.

Burrows M (1996) The neurobiology of an insect brain. New York: Oxford UP.

Byers D, Davis RL, Kiger Jr JA (1981) Defect in cyclic AMP phosphodiesterase due to the dunce mutation of learning in *Drosophila melanogaster*. Nature 289:79–81.

Choi JC, Park D, Griffith LC (2004) Electrophysiological and morphological characterization of identified motor neurons in the Drosophila third instar larva central nervous system. J Neurophysiol 91:2353–2365.

Cohan CS, Connor JA, Kater SB (1987) Electrically and chemically mediated increases in intracellular calcium in neuronal growth cones. J Neurosci 7:3588–3599.

Crittenden JR, Skoulakis EM, Han KA, Kalderon D, Davis RL (1998) Tripartite mushroom body architecture revealed by antigenic markers. Learn Mem 5:38–51.

Davis GW, Schuster CM, Goodman CS (1996) Genetic dissection of structural and functional components of synaptic plasticity. III. CREB is necessary for presynaptic functional plasticity. Neuron 17:669–679.

Dudai Y, Jan YN, Byers D, Quinn WG, Benzer S (1976) dunce, a mutant of *Drosophila* deficient in learning. Proc Natl Acad Sci USA 73:1684–1688.

Fields RD, Neale EA, Nelson PG (1990) Effects of patterned electrical activity on neurite outgrowth from mouse sensory neurons. J Neurosci 10:2950–2964.

Ganetzky B, Wu CF (1983) Neurogenetic analysis of potassium currents in *Drosophila*: synergistic effects on neuromuscular transmission in double mutants. J Neurogenet 1:17–28.

Gho M, Ganetzky B (1992) Analysis of repolarization of presynaptic motor terminals in Drosophila larvae using potassium-channel-blocking drugs and mutations. J Exp Biol 170:93–111.

Gomez TM, Spitzer NC (1999) In vivo regulation of axon extension and pathfinding by growth-cone calcium transients. Nature 397:350–355.

Groh C, Tautz J, Rossler W (2004) Synaptic organization in the adult honey bee brain is influenced by brood-temperature control during pupal development. Proc Natl Acad Sci USA 101:4268–4273.

Grynkiewicz G, Poenie M, Tsien RY (1985) A new generation of Ca2+ indicators with greatly improved fluorescence properties. J Biol Chem 260:3440–3450.

Haghighi AP, McCabe BD, Fetter RD, Palmer JE, Hom S, Goodman CS (2003) Retrograde control of synaptic transmission by postsynaptic CaMKII at the *Drosophila* neuromuscular junction. Neuron 39:255–267.

Haugland FN, Wu CF (1990) A voltage-clamp analysis of gene-dosage effects of the Shaker locus on larval muscle potassium currents in *Drosophila*. J Neurosci 10:1357–1371.

Heisenberg M, (1998) What do the mushroom bodies do for the insect brain? An introduction. Learn Mem 5:1–10.

Hong ST, Bang S, Paik D, Kang J, Hwang S, Jeon K, Chun B, Hyun S, Lee Y, Kim J (2006) Histamine and its receptors modulate temperature-preference behaviors in *Drosophila*. J Neurosci 26:7245–7256.

Ito K, Hotta Y (1992) Proliferation pattern of postembryonic neuroblasts in the brain of *Drosophila melanogaster*. Dev Biol 149:134–148.

Ito K, Awano W, Suzuki K, Hiromi Y, Yamamoto D (1997) The *Drosophila* mushroom body is a quadruple structure of clonal units each of which contains a virtually identical set of neurones and glial cells. Development 124:761–771.

Jones JC, Helliwell P, Beekman M, Maleszka R, Oldroyd BP (2005) The effects of rearing temperature on developmental stability and learning and memory in the honey bee, *Apis mellifera*. J Comp Physiol [A] 191:1121–1129.

Kazama H, Morimoto-Tanifuji T, Nose A (2003) Postsynaptic activation of calcium/calmodulin-dependent protein kinase II promotes coordinated pre- and postsynaptic maturation of *Drosophila* neuromuscular junctions. Neuroscience 117:615–625.

Kazama H, Nose A, Morimoto-Tanifuji T (2007) Synaptic components necessary for retrograde signaling triggered by calcium/calmodulin-dependent protein kinase II during synaptogenesis. Neuroscience 145:1007–1015.

Kim YT, Wu CF (1996) Reduced growth cone motility in cultured neurons from *Drosophila* memory mutants with a defective cAMP cascade. J Neurosci 16:5593–5602.

Kimura KD, Miyawaki A, Matsumoto K, Mori I (2004) The *C. elegans* thermosensory neuron AFD responds to warming. Curr Biol 14:1291–1295.

Kirov SA, Petrak LJ, Fiala JC, Harris KM (2004) Dendritic spines disappear with chilling but proliferate excessively upon rewarming of mature hippocampus. Neuroscience 127:69–80.

Klyachko VA, Stevens CF (2006) Temperature-dependent shift of balance among the components of short-term plasticity in hippocampal synapses. J Neurosci 26:6945–6957.

Kushmerick C, Renden R, von Gersdorff H (2006) Physiological temperatures reduce the rate of vesicle pool depletion and short-term depression via an acceleration of vesicle recruitment. J Neurosci 26:1366–1377.

Lau PM, Zucker RS, Bentley D (1999) Induction of filopodia by direct local elevation of intracellular calcium ion concentration. J Cell Biol 145:1265–1275.

Lee T, Lee A, Luo L (1999) Development of the *Drosophila* mushroom bodies: sequential generation of three distinct types of neurons from a neuroblast. Development 126:4065–4076.

Lee Y, Lee J, Bang S, Hyun S, Kang J, Hong ST, Bae E, Kaang BK, Kim J (2005) Pyrexia is a new thermal transient receptor potential channel endowing tolerance to high temperatures in *Drosophila melanogaster*. Nat Genet 37:305–310.

Livingstone MS, Sziber PP, Quinn WG (1984) Loss of calcium/calmodulin responsiveness in AC of rutabaga, a *Drosophila* learning mutant. Cell 37:205–215.

Liu G, Seiler H, Wen A, Zars T, Ito K, Wolf R, Heisenberg M, Liu L (2006) Distinct memory traces for two visual features in the *Drosophila* brain. Nature 439:551–556.

McCade BD, Marques G, Haghighi AP, Fetter RD, Crotty ML, Haerry TE, Goodman CS, O'Connor MB (2003) The BMP homolog Gbb provides a retrograde signal that regulates synaptic growth at the *Drosophila* neuromuscular junction. Neuron 39:241–254.

O'Dell KM, Armstrong JD, Yang MY, Kaiser K (1995) Functional dissection of the *Drosophila* mushroom bodies by selective feminization of genetically defined subcompartments. Neuron 15:55–61.

Peng IF, Wu CF (2007a) Differential contributions of Shaker and Shab K+ currents to neuronal firing patterns in *Drosophila*. J Neurophysiol 97:780–794.

Peng IF, Wu CF (2007b) Drosophila cacophony channels: a major mediator of neuronal Ca2+ currents and a trigger for K+ channel homeostatic regulation. J Neurosci 27:1072–1081.

Petersen SA, Fetter RD, Noordermeer JN, Goodman CS, DiAntonio A (1997) Genetic analysis of glutamate receptors in *Drosophila* reveals a retrograde signal regulating presynaptic transmitter release. Neuron 19:1237–1248.

Popov VI, Bocharova LS (1992) Hibernation-induced structural changes in synaptic contacts between mossy fibres and hippocampal pyramidal neurons. Neuroscience 48:53–62.

Popov VI, Bocharova LS, Bragin AG (1992) Repeated changes of dendritic morphology in the hippocampus of ground squirrels in the course of hibernation. Neuroscience 48:45–51.

Renger JJ, Yao WD, Sokolowski MB, Wu CF (1999) Neuronal polymorphism among natural alleles of a cGMP-dependent kinase gene, foraging, in *Drosophila*. J Neurosci 19:RC28(1–8).

Renger JJ, Ueda A, Atwood HL, Govind CK, Wu CF (2000) Role of cAMP cascade in synaptic stability and plasicity: ultrastructural and physiological analyses of individual synaptic boutons in *Drosophila* memory mutants. J Neurosci 20:3980–3992.

Rosenzweig M, Brennan KM, Tayler TD, Phelps PO, Patapoutian A, Garrity

PA (2005) The Drosophila ortholog of vertebrate TRPA1 regulates thermotaxis. Genes Dev 19:419–424.
Saito M, Wu CF (1991) Expression of ion channels and mutational effects in giant *Drosophila* neurons differentiated from cell division-arrested embryonic neuroblasts. J Neurosci 11:2135–2150.
Salvaterra PM, Bournias-Vardiabasis N, Nair T, Hou G, Lieu C (1987) In vitro neuronal differentiation of *Drosophila* embryo cells. J Neurosci 7:10–22.
Samuel AD, Silva RA, Murthy VN (2003) Synaptic activity of the AFD neuron in Caenorhabditis elegans correlates with thermotactic memory. J Neurosci 23:373–376.
Schuster CM, Davis GW, Fetter RD, Goodman CS (1996) Genetic dissection of structural and functional components of synaptic plasticity. II. Fasciclin II controls presynaptic structural plasticity. Neuron 17:655–667.
Sigrist SJ, Reiff DF, Thiel PR, Steinert JR, Schuster CM (2003) Experience-dependent strengthening of *Drosophila* neuromuscular junctions. J Neurosci 23:6546–6556.
Singh S, Wu CF (1999) Ionic currents in larval muscles of *Drosophila*. Int Rev Neurobiol 43:191–220.
Steinert JR, Kuromi H, Hellwig A, Knirr M, Wyatt AW, Kidokoro Y, Schuster CM (2006) Experience-dependent formation and recruitment of large vesicles from reserve pool. Neuron 50:723–733.
Tautz J, Maier S, Groh C, Rossler W, Brockmann A (2003) Behavioral performance in adult honey bees is influenced by the temperature experienced during their pupal development. Proc Natl Acad Sci USA 100:7343–7347.
Tracey WD, Jr., Wilson RI, Laurent G, Benzer S (2003) painless, a *Drosophila* gene essential for nociception. Cell 113:261–273.
Tully T, Quinn WG (1985) Classical conditioning and retention in normal and mutant *Drosophila melanogaster*. J Comp Physiol [A] 157:263–277.
Wan YH, Jian Z, Wang WT, Xu H, Hu SJ, Ju G (2006) Short-term plasticity at primary afferent synapse in rat spinal dorsal horn and its biological function. Neurosignals 15:74–90.
Wang J, Renger JJ, Griffith LC, Greenspan RJ, Wu CF (1994) Concomitant alterations of physiological and developmental plasticity in *Drosophila* CaM kinase II-inhibited synapses. Neuron 13:1373–1384.
Williams DA, Fogarty KE, Tsien RY, Fay FS (1985) Calcium gradients in single smooth muscle cells revealed by the digital imaging microscope using Fura-2. Nature 318:558–561.
Wu CF, Haugland FN (1985) Voltage clamp analysis of membrane currents in larval muscle fibers of *Drosophila*: alteration of potassium currents in Shaker mutants. J Neurosci 5:2626–2640.
Wu CF, Ganetzky B, Haugland FN, Liu AX (1983) Potassium currents in Drosophila: different components affected by mutations of two genes. Science 220:1076–1078.
Wu CF, Sakai K, Saito M, Hotta Y (1990) Giant *Drosophila* neurons differentiated from cytokinesis-arrested embryonic neuroblasts. J Neurobiol 21:499–507.
Yang MY, Armstrong JD, Vilinsky I, Strausfeld NJ, Kaiser K (1995) Subdivision of the *Drosophila* mushroom bodies by enhancer-trap expression patterns. Neuron 15:45–54.
Yao WD, Wu CF (1999) Auxiliary hyperkinetic beta subunit of K+ channels: regulation of firing properties and K+ currents in *Drosophila* neurons. J Neurophysiol 81:2472–2484.
Yoshihara M, Adolfsen B, Galle KT, Littleton JT (2005) Retrograde signaling by Synaptotagmin 4 induces presynaptic release and synapse-specific growth. Science 310:858–863.
Zhao ML, Wu CF (1997) Alterations in frequency coding and activity dependence of excitability in cultured neurons of *Drosophila* memory mutants. J Neurosci 17:2187–2199.
Zhao ML, Sable EO, Iverson LE, Wu CF (1995) Functional expression of Shaker K+ channels in cultured *Drosophila*"giant" neurons derived from Sh cDNA transformants: distinct properties, distribution, and turnover. J Neurosci 15:1406–1418.
Zheng JQ (2000) Turning of nerve growth cones induced by localized increases in intracellular calcium ions. Nature 403:89–93.
Zhong Y, Wu CF (1993) Modulation of different K+ currents in *Drosophila*: a hypothetical role for the Eag subunit in multimeric K+ channels. J Neurosci 13:4669–4679.
Zhong Y, Wu CF (2004) Neuronal activity and adenylyl cyclase in environment-dependent plasticity of axonal outgrowth in *Drosophila*. J Neurosci 24:1439–1445.
Zhong Y, Budnik V, Wu CF (1992) Synaptic plasticity in *Drosophila* memory and hyperexcitable mutants: role of cAMP cascade. J Neurosci 12:644–651.